Journal of Natural Gas Science and Engineering 96 (2021) 104275

Contents lists available at ScienceDirect

Journal of Natural Gas Science and Engineering

journal homepage: www.elsevier.com/locate/jngse

Modeling temporal variability in the surface expression above a methane leak: The ESCAPE model

Stuart N. Riddick [a,*], Clay S. Bell [a], Aidan Duggan [a], Timothy L. Vaughn [a], Kathleen M. Smits [b], Younki Cho [b], Kristine E. Bennett [a], Daniel J. Zimmerle [a]

[a] The Energy Institute, Colorado State University, CO, USA
[b] Department of Civil Engineering, The University of Texas at Arlington, TX, USA

ARTICLE INFO

Keywords:
Methane
Leak
Pipeline
Detection
Surface
Misdiagnosis

ABSTRACT

Leaks in natural gas distribution networks are often initially detected by odor and then localized during operators' walking surveys. The size of the enhancement detected and the leak's proximity to infrastructure are used to determine leak severity of the leak and how quickly it is repaired. Methane (CH_4) enhancements on the surface above the leak change with atmospheric conditions, but currently the leak severity assessment is made without considering the environmental conditions and could result in misdiagnosis of the leak. This study has developed the "ESCAPE" model, a tool that can be used to estimate CH_4 enhancements on the surface above a leak using meteorological and leak data as input. Surface CH_4 concentrations calculated using the ESCAPE model agrees well with measurements made during controlled experiments ($m = 0.95$ and $R^2 = 0.95$). This study highlights the effect of micrometeorology on gas transport from the surface to the atmosphere, where the surface and the atmospheric conditions have the largest effect on the flux. Here, recommendations are made to improve industry best practices, including recording the meteorological conditions at the time of the leak detection, avoiding walking surveys on days where there are strong winds or strong solar irradiance and that known leak locations should be revisited and measured in different conditions. Mitigating CH_4 emissions from the gas distribution network is a cost-effective and economically realistic target. Distribution operators can be directed by the output of ESCAPE model to correctly identify and repair the largest distribution leaks and could reduce annual CH_4 emissions by 0.69 Tg, this may go some way to reducing energy sector emissions in accordance with the Paris Agreement.

1. Introduction

Natural gas transportation is generally structured into three *sectors*. *Gathering* pipelines collect gas from production wells and well pads and transport gas to processing plants and transmission systems. *Transmission* pipelines carry gases at high pressure (3500 to 9600 kPa) over continental distances, as well as integrating gas storage, electrical power plants, and industrial facilities. Finally, *distribution* pipelines transport gas from transmission systems to residential and commercial end users, typically operating at middle and lower pressures (1.5–2000 kPa); distribution mains in residential areas typically operate below 400 kPa. Gas transported in transmission and distribution systems has a generally standardized composition consisting primarily of methane with 0–10% ethane and low concentration of other hydrocarbons. In contrast, gathering systems carry a wide range of gas compositions, with methane concentrations as low as 50% in some systems. Only distribution systems odorize gas with mercaptan at concentrations less than 10 ppm and typically between 3 and 4 ppm (Rosemarie Halchuk, XCEL Energy, pers. comm.), although gathering system gas may contain naturally occurring aromatic compounds.

Gas pipelines may leak due to corrosion, external stressors, or other factors. Failure of high-pressure pipelines typically result in cascade failures that are detected, controlled, and repaired quickly. In contrast, smaller leaks from distribution networks are more difficult to detect and may go unnoticed without targeted leak detection surveys. While these leaks release substantially less gas than high pressure pipelines, proximity to structures may create equally hazardous conditions when gas migrates into enclosed spaces, such as storm drains, basements, foundations, or utility conduits. Methane is explosive at concentrations between 4 and 17%, is lighter than air, and even small CH_4 leaks can

* Corresponding author.
E-mail address: Stuart.Riddick@colostate.edu (S.N. Riddick).

https://doi.org/10.1016/j.jngse.2021.104275
Received 7 May 2021; Received in revised form 24 September 2021; Accepted 28 September 2021
Available online 1 October 2021

collect to explosive concentrations in spaces where the gas' vertical movement is blocked. Gas leaks have resulted in an average of 155 explosions or fires per year annually in the USA (PHMSA, 2021). It is estimated that in Paris 56% of the detectable emissions from the ground result from natural gas distribution network emissions with total emissions of ~1 Gg per year (Defratyka et al., 2021). In 2020, there were an estimated 630,000 leaks in U.S. distribution mains, resulting in methane emissions of 0.69 Tg per year (Weller et al., 2020). Leaks from the gas distribution network contribute to the increase in atmospheric CH_4 growth from 1775 ppb in 2006 to 1850 ppb in 2017 (Nisbet et al., 2019), are a fugitive CH_4 source that could be mitigated by a targeted approach to identify and repair the largest leaks (Maazallahi et al., 2020; Weller et al., 2020), and have been identified as a good target for reduction of CH_4 emissions from fossil fuels if the Paris Agreement is to be met (Nisbet et al., 2019).

While many leaks in the distribution network are identified by the public reporting an odor, walking surveys are routinely used by distribution companies to locate leaks. Mercaptan can be detected by the human nose to concentrations as low as 1 ppb and, in lieu of additional instrumentation, leaks may be detected by the odorant alone in many contexts when concentrations of natural gas are above 100 ppm. However, this is a presence/absence observation and surveyors use gas sensors to quantitatively measure hydrocarbon concentration enhancements at the surface, and in turn, assess the severity of the leak. The severity is determined by considering the estimated size and concentration of the leak and its proximity to structures. One potential problem with walking surveys is that the collection of gas at the surface is a dynamic process, and changes in subsurface and atmospheric conditions can change surface concentrations significantly (Cho et al., 2020; Ulrich et al., 2019). A recent study used a walking survey to detect methane enhancements of up to 100 ppb at the Munich Oktoberfest in 2018 (Chen et al., 2020).

There are a variety of technologies that can be used to detect oil, gas, produced water and condensate leaks from belowground sources. Solutions include fixed sensor systems that are installed inside or outside the pipe as well as internal mobile tools that are deployed after pipeline installation. A comprehensive analysis of such detection technologies is provided by Shaw et al. (2012), Henrie et al. (2016) and Zimmerle et al. (2017). Specific to leak detection for distribution lines, above ground gas leak detection methods are primarily used. Walking surveys are the primary method used for leak detection. Some companies are experimenting with driving surveys using trace gas analyzers. Aerial or driving surveys are typically utilized for leak detection on gas transmission mains where long rights-of-way make these methods more practical. Transient tests, such as those used in water mains, are not typically applied in gas pipelines where the flow is compressible.

To better understand variability in surface CH_4 concentrations, an Ohm's Law analogy can be used to predict the size of gas emissions from the surface (Neirynck et al., 2007; Nemitz et al., 2000; Riddick et al., 2017; Sutton et al., 1998; Zhang et al., 2002). The flow of gas from the leak to the atmosphere (Q) can be calculated from the difference in gas mixing ratios between the leak (X_l) and the atmosphere (X_{at}) and the combined resistance to gas flow in the soil (R_s) and the atmosphere (R_{at}) (Fig. 1; Equation (1)). Here, we acknowledge that soil is not only resistant to CH_4 flow but also a sink as methanotrophic bacteria can consume the gas as it passes through the soil, given sufficient residence time.

$$Q_x = \frac{(\chi_l - \chi_{at})}{(R_{at} + R_s)} \quad \text{(Equation 1)}$$

The R_{at} is a function of wind speed and atmospheric stability, where the atmospheric stability is a function of the wind speed, temperature gradient from ground to ambient air and solar irradiance, and R_{at} becomes less, i.e. it is easier for air to travel vertically, in higher wind speeds or with more solar heating of the ground (Seinfeld and Pandis, 2016). It is expected that the surface concentration (X_s) will become lower as R_{at} decreases, i.e. in stronger wind in an unstable atmosphere, X_s will become higher as R_{at} increases, i.e. in low wind in a very stable atmosphere.

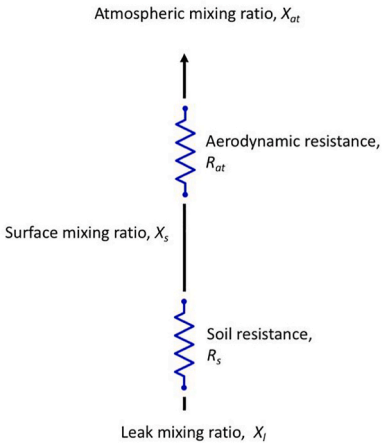

Fig. 1. Resistance analogy of a subsurface leak.

Relative to equipment leaks in upstream sectors and leaks in transmission lines, leaks from the distribution network are small. A recent study of 230 distribution leaks across the USA found that 90% were less than 66 g CH_4 h^{-1} and 50% were less than 4 g CH_4 h^{-1} (Lamb et al., 2015) – walking surveys may not detect leaks of this size. For example, a measurement study observed CH_4 mixing ratios of 2000 ppm directly above a relatively large leak (400 g CH_4 h^{-1}) (Ulrich et al., 2019) in neutral wind conditions with Pasquill Gifford stability class D and wind speed 3 m s^{-1}. If measurements were to take place over a smaller leak, e.g. 100 times smaller 4 g CH_4 h^{-1}, during a period of increased wind speed and in less stable conditions, the gas sensors used in walking surveys would likely not detect the resulting maximum surface CH_4 concentration. Additionally, the locational accuracy of pipelines is not precise, often resulting in surveyors sensing some distance (up to several meters) from the centerline of the pipe.

This study focusses on distribution system leaks and aims to identify the effects of atmospheric variability on the surface presentation of the leak which will lead to a better understanding of observed concentrations mapped during typical walking surveys. Explicitly, the study's aims are: 1) Use the resistance analogy above to create a dynamic process-based model to calculate CH_4 at the surface above a leak; 2) Validate the modelled surface CH_4 mixing ratios by comparing them to measurements made on the surface above gas leaks of known release rates in different meteorological and micrometeorological conditions; and 3) Investigate the possibilities of false signaling during walking surveys, i.e. are there conditions in which large leaks have a very small surface concentration and conversely conditions where small leaks have large surface enhancements.

2. Methods

2.1. Surface concentration modeling

2.1.1. Below surface gas flow rates

For the small leaks considered here, below ground gas flow is limited by diffusion – advective transport impacts only a small region at the source of the leak – where the rate of diffusion of a gas through a porous soil is a function of the gas concentration gradient (Jury et al., 1991; Wang et al., 2014) and microbial methanotrophic uptake of CH_4. The diffusive flow can be calculated using Fick's law (Equation (2)), where the diffusion flux at distance x from the leak (f_{dx}, g m^{-2} s^{-1}) is the product of the concentration gradient at x from the leak (∇C_x, g m^{-4}) and the diffusion coefficient (D_p, m^2 s^{-1}) and gas flow from the leak to the surface can be calculated by complex numerical simulations (Bu

et al., 2021; Hou and Yuan, 2021; Wang et al., 2021).

$$f_{dx} = -D_p.\nabla C_x \quad \text{(Equation 2)}$$

However, it is unlikely that a walking surveyor will be able to adequately measure or estimate any of variables used in the simulations, and instead, we take a zeroth order approach to estimating the gas flow to support development of a practical model can be used in the field to identify the severity of the leak. Here, we model below-surface flow making five main assumptions: 1) soil properties impacting diffusion are uniform throughout the modelled domain; 2) gas flows (F, g s^{-1}) in straight lines from the leak to the surface and inversely proportional to the resistance of flow ($F_x \propto \frac{1}{R_{sx}}$); 3) consistent with Fick's law, the resistance of flow is proportional to the distance the gas has to travel ($R_{sx} \propto D_x$) (Fig. 2); 4) the emission at perpendicular distance x (Q_x, g s^{-1}) can be scaled to the actual size of the leak; and 5) the gas is in steady state and can only vent to the atmosphere – i.e. there are no nearby enclosed spaces into which the gas may migrate. Note that this model does not include different surface covers; e.g. impermeable layers such as concrete or asphalt that may cause gas to migrate long distances to cracks or edges before reaching an active atmospheric interface. This simplified structure provides a useful tool for understanding the physics of underground gas migration, suitable for translation into field practices.

Using the assumptions set out above, we define the surface flux at distance x (F_x, g m^{-2} s^{-1}) as a function of the emission at x (Q_x, g s^{-1}), the sum of all emission rates ($\sum_{x=0}^{\infty} Q_x$, g s^{-1}), the total leak rate (Q_T, g s^{-1}) and the area of the surface expression between perpendicular steps (A_x, m^2) (Equation (3)). In this study, we define $x = 0$ as the point on the ground surface, immediately above the pipe and we increase x in steps of 0.5 m. The value of Q_x is calculated from the perpendicular distance from the leak (x, m), the depth of the leak (d, m) and an undefined variable (V) that accounts of the contributions of ∇C_x and D_p and cancels out in Equation (3).

$$F_x = \frac{Q_T}{A_x}.\frac{Q_x}{\sum_{x=0}^{\infty} Q_x}, where, Q_x = \frac{V}{\sqrt{(x^2+d^2)}} and A_x = \pi\left(\left(x+\frac{x}{2}\right)^2 - \left(x-\frac{x}{2}\right)^2\right) \quad \text{(Equation 3)}$$

2.1.2. Above surface resistance

The total atmospheric resistance (R_{at}, m s^{-1}) is the summation of the boundary layer resistance (R_b, m s^{-1}) and the aerodynamic resistance (R_a, m s^{-1}). The boundary layer resistance (R_b, m s^{-1}) describes how the gas diffuses through the quasi-laminar sub-layer of vegetation at the surface (Equation (4)). This is the product of the friction velocity (u^*, m s^{-1}) and the boundary layer Stanton number (B) (Nemitz et al., 2000; Sutton et al., 1993).

$$R_b = (Bu^*)^{-1} \quad \text{(Equation 4)}$$

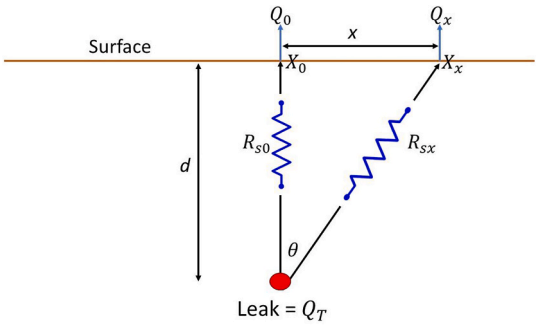

Fig. 2. Gas flow in soil showing assumptions made by the model: 1) gas flows in straight lines from the leak to the surface; 2) gas flow is inversely proportional to the resistance of flow; and 3) the resistance of flow is proportional to the distance the gas has to travel.

The aerodynamic resistance (R_a, m s^{-1}) is a function (Equation (5)) of the roughness length (z_0, m), the displacement length (z_d, m), the Monin-Obukhov length (L, m), the von Karman constant ($k = 0.41$), the wind speed (u, m s^{-1}) and a stability correction function (ψ_m) (Seinfeld and Pandis, 2016). The stability correction function can be calculated for both stable and unstable conditions, these functions are explicitly defined in Equations (6) and (7), respectively. Stable conditions occur, and R_a increases, during periods of low wind and low solar heating. Unstable conditions occur during period of high wind and high solar heating, causing gases to be quickly moved from the surface into the atmosphere.

$$R_a = \frac{\left[ln\left(\frac{z-z_d}{z_0}\right) - \psi_m\left(\frac{z-z_d}{L}\right)\right]^2}{k^2 u} \quad \text{(Equation 5)}$$

Stable conditions

$$\psi_m\left(\frac{z}{L}\right) = -\frac{5z}{L} \quad \text{(Equation 6)}$$

Unstable conditions:

$$\psi_m\left(\frac{z}{L}\right) = 2ln\left(\frac{1+X}{2}\right) + ln\left(\frac{1+X^2}{2}\right) - 2tan^{-1}(X) + \frac{\pi}{2}, where X = \left(1-16\frac{z}{L}\right)^{\frac{1}{4}} \quad \text{(Equation 7)}$$

2.1.3. Modeling surface mixing ratios

Using the Ohm's Law analogy (Equation (8)) we then calculate the surface mixing ratio (X_x, ppm) from F_x (Equation (3)) and R_{at} and assume a background atmospheric CH_4 mixing ratio (X_{at}) of 1.88 ppm (Dlugokencky, 2020). Henceforth, this model will be referred to as the ESCAPE (Estimating the Surface Concentration Above Pipeline Emissions) model.

$$F_x = \frac{(\chi_x - \chi_{at})}{R_{at}} \quad \text{(Equation 8)}$$

2.2. Validating the ESCAPE model

2.2.1. Input data to ECSAPE model

The ESCAPE model requires time varying data inputs of wind speed and Pasquill Gifford Stability Class (PGSC), where the PGSC is a function of the wind speed and solar irradiance (Seinfeld and Pandis, 2016). Wind speed, roughness length and Monin-Obukhov length were measured onsite using a Model 81,000 anemometer (R. M. Young, Traverse City, USA). Leak rates were pre-determined and controlled by regulating the pressure upstream of a precision orifice at the Methane Emission Technology Evaluation Center (METEC) at Colorado State University in Fort Collins, USA (see (Bell et al., 2020) for a control system description). The leaks were simulated using 0.25" stainless steel tubing installed 1 m below the soil at METEC 12 months previously (Mitton, 2018).

2.2.2. Measuring surface enhancements

To validate ESCAPE model output, CH_4 mixing ratio measurements spatially matching the modelled estimates were made on the surface within the vicinity of the leak location, in two steps. First, a Bascom-Turner Gas Rover (Bascom Turner Instruments VGI-201, accuracy of 2% reading ± 20 ppm at 1 Hz) was used to find the highest concentration. This position was taken as the reference point for the rest of the measurements and referred to henceforth as the "focus". A radial grid, separated by 45° using a compass, was then laid out using the focus as the center with measurement points marked every half meter. At a minimum, 24 surface measurements were taken for each experiment.

Second, surface measurements were conducted by pressing the rubber cup of the Gas Rover lightly onto the surface at each radial position for 2 min. To reduce bias as the sensors equilibrated, the mixing

ratio measurements used for this study were taken as the average of the last minute of each measurement. In addition to CH_4 mixing ratio data at the ground/air interface, wind speed, wind direction, air temperature, surface temperature, atmospheric pressure, roughness length and the Monin-Obukhov length were all measured at the site, 1.5 m above ground level (AGL). Surface mixing ratio measurements were made for 24 leaks, ranging from 4 to 270 g h^{-1}, after steady state emission had occurred (at least 24-h after the leak was initiated). In addition, to investigate the performance of the ESCAPE model tests were performed under various meteorological conditions.

As these experiments were conducted using a single belowground soil test bed, the effects of soil type were not investigated. For direct comparison with modelled CH_4 surface mixing ratios, the average of the eight radial mixing ratios at the same distance were used. The gradient of the line of best fit between modelled and measured mixing ratios, the coefficient of determination (R^2) and the p-value were used as metrics to ascertain how well the ESCAPE model predicts CH_4 surface mixing ratios at distances from the focus.

2.3. Testing surface enhancement extremes

To investigate the possibility of false signaling during walking surveys, we used the ESCAPE model to predict how surface mixing ratios changed in climatic conditions at the extreme ranges of the modeling input. The two emissions scenarios used were: a larger than average leak of 80 g h^{-1} and a small leak of 4 g h^{-1}. Wind speeds varied from 0.5 to 7.5 m s^{-1}, PGSC varied from A to G, Monin-Obukhov lengths from −11 to 5 m and roughness lengths from 0.0001 m (snow) to 0.1 m (wheat fields) (Seinfeld and Pandis, 2016).

3. Results

3.1. Validation of modelled surface enhancements

3.1.1. Surface enhancement measurements

Measured CH_4 surface mixing ratios were highest directly above the leak. High observable mixing ratios extend to a radius of around 1 m from above the leak, maximum 20,000 ppm, and mixing ratios quickly decrease to background. Methane enhancements on the surface are undetectable more than 4.5 m from the leak (Table 1) for any leak size. It

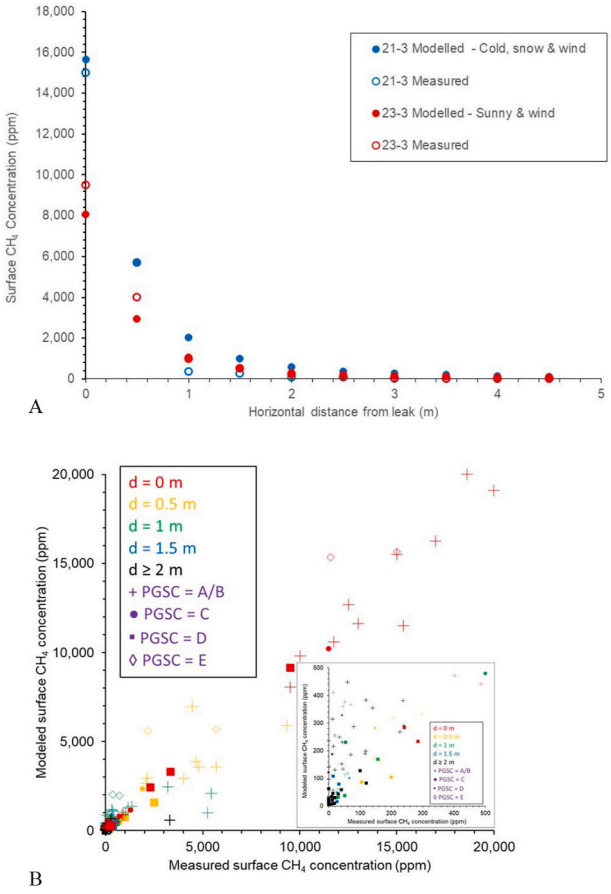

Fig. 3. Surface CH_4 mixing ratios above a larger than average leak, 80 g h^{-1} on the May 2, 2020.

Table 1
Maximum CH_4 mixing ratio predicted by the ESCAPE model (Model. CH_4 max (ppm)), maximum measured CH_4 mixing ratio (Meas. CH_4 max (ppm)) distance from the focus that an enhancement can be detected (En. Radius), R^2 between modelled and measured values at distances from the leak and the gradient (m) of the line of best fit between modelled and measured values at distances from the leak. PGSC denotes the Pasquill-Gifford Stability Class and WS is the wind speed.

Date	Leak rate (g h-1)	WS (m s^{-1})	PGSC	Model CH_4 max (ppm)	Meas. CH_4 max (ppm)	En. Radius (m)	R^2	m
May 02, 2020	4	2.2	B	350	486	1.5	0.95	1.28
May 03, 2020	4	1.2	A	712	840	1.5	0.98	1.18
May 05, 2020	4	1.9	A	370	402	1.5	0.93	1.08
May 14, 2020	4	1.7	C	606	707	1.5	0.98	1.16
May 16, 2020	4	3.1	D	222	241	1.5	0.83	1.06
May 19, 2020	4	1.3	A	686	897	2.0	0.99	1.30
May 20, 2020	4	4.5	D	264	285	1.5	0.98	1.05
May 02, 2020	20	1.2	B	11,758	13,000	2.0	0.98	1.09
May 03, 2020	20	1.1	A	12,827	12,500	1.5	0.98	0.96
May 05, 2020	20	0.9	A	15,677	15,000	1.0	0.88	0.92
May 14, 2020	20	1.7	C	10,316	11,500	1.5	0.98	1.09
May 16, 2020	20	6.1	D	2437	2300	2.5	0.94	0.91
May 20, 2020	20	3.0	D	3352	3352	1.5	0.93	0.98
May 23, 2020	20	1.2	A	9140	9500	3.5	0.99	1.04
January 19, 1900	40	0.7	A	16,245	17,000	3.0	0.90	1.03
March 17, 2020	80	2.0	E	11,989	11,570	3.0	0.98	0.96
March 18, 2020	80	2.7	B	10,212	10,000	2.5	0.98	0.97
March 21, 2020	80	2.0	E	16,260	15,000	2.5	0.99	0.92
March 23, 2020	80	3.0	B	9247	9500	2.5	0.94	0.99
March 25, 2020	80	2.5	B	11,029	11,750	3.0	0.99	1.06
May 21, 2020	70	2.6	A	19,106	20,000	3.0	0.98	1.03
May 26, 2020	120	1.0	C	1282	1150	2.5	0.97	1.05
June 02, 2020	180	1.3	B	15,333	11,500	3.5	0.99	1.27
June 04, 2020	270	2.2	B	18,611	20,000	4.5	0.99	0.90

is important to note that these are only for the conditions tested (e.g. Fig. 3).

The initial observation provides a key input for walking surveys: The centerline of the pipeline needs to be located to ≤ 2 meters for practical surveys to capture leaks of 20 g CH_4 h^{-1}. Recollecting that the tests performed here were in relatively porous soil, no surface cover, over a relatively shallow leak location, the above guidance should be considered a maximum for pipeline location accuracy.

3.1.2. ESCAPE model output

Using the ESCPAE model, X_x is calculated for perpendicular distances from the focus for the meteorological conditions observed in Section 3.1.1. As examples, modelled surface CH_4 mixing ratios (Fig. 4A) for a (large) 80 g h^{-1} leak 0.5 m below the surface, measured at $z_0 = 1$ *cm* AGL, in a high stability, PGSC E, (solid blue points) show a maximum calculated mixing ratio of 15,644 ppm (Table 1) while that maximum mixing ratio predicted for unstable conditions, PGSC B, (solid red points) is 8046 ppm. In both the stable and unstable scenarios, the CH_4 mixing ratios predicted by the ESCAPE model fall to less than 2000 ppm 1 m away from the focus and less than 100 ppm at 3 m from the focus. Both stable and unstable examples are in good agreement with measured data with an R^2 of 0.95 and 0.96, respectively.

When mixing ratios generated by the ESCAPE model are compared against measured mixing ratios at the same distance from the focus in all environmental conditions, we find that there is good agreement with R^2 of 0.95 (Fig. 4B; Table 1). The p-values for each of the modelled/measured datasets are less than 0.001. The ESCAPE model appears to be less accurate during low wind, < 2 m s^{-1}, conditions in both stable and unstable atmospheres, it overpredicts surface mixing ratios in stable conditions, m of 0.74 in PGSC E stability, while underpredicting in unstable conditions, m of 1.30 in PGSC B conditions. Despite this, the ESCAPE model appears to capture the shape of the changing CH_4 surface mixing ratios with distance from the focus (Fig. 4A).

Data presented from multiple sizes of leaks in different atmospheric conditions show that, in general, surface CH_4 mixing ratios above the focus are lower in stable conditions and also in high winds (Table 1),

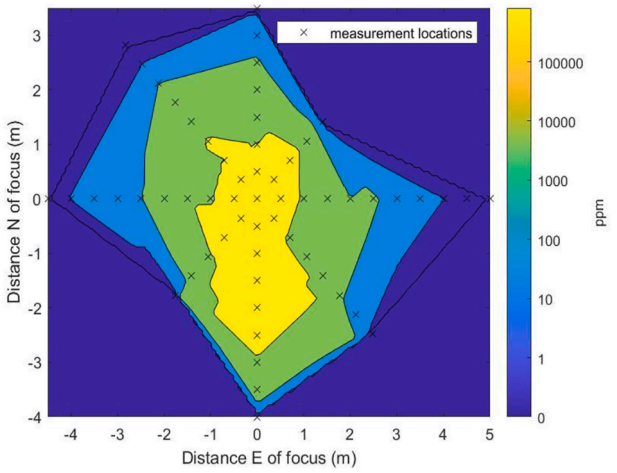

Fig. 4. A) Surface methane mixing ratios (solid points) as calculated by the ESCAPE model for a 80 g h^{-1} leak 0.5 m below the surface in a high stability (21/3/20) and unstable condition (23/3/20). Matching measured methane mixing ratios are presented (hollow points). B) Comparison between measured methane surface mixing ratio and matching mixing ratios calculated by the ESCAPE model at distances from the leak focus in different meteorological and micrometeorological conditions. Crosses indicate measurements made in PGSC A/B conditions, circles in PGSC C, squares in PGSC D and diamonds in PGSC E. Red symbols indicate measurements above the leak, orange symbols are 0.5 m from the leak, green symbols are 1 m, blue symbols are 1.5 m and black symbols were greater than 1.5 m away. Inset plot focusses on lower concentration region of outer plot.

with the lowest modelled/measured mixing ratio 234/285 ppm, during a 7.1 m s^{-1} wind event in PGSC class D on the 20/5/20. Higher surface CH_4 mixing ratios above the focus were observed above the same leak, 4 g h^{-1}, during low wind and stable conditions, with the highest modelled/measured mixing ratio 910/840 ppm, on the 03/05/20 when the wind was 1.2 m s^{-1} and the PGSC was A.

3.2. Extreme scenarios

3.2.1. Large leaks with small surface expression

Taking the example of an above average leak of 80 g h^{-1} that is 50 cm below the surface, the surface CH_4 mixing ratio above the focus, as calculated by the ESCAPE model, is smallest when the surface roughness is largest, the wind speed is high and the atmosphere is more unstable (Fig. 5). When all of these variables are tuned in the ESCAPE model to these extremes, where z_0 is 0.1 m (e.g. wheat field), wind speed is 7.5 m s^{-1} and a stability of PGSC A, the surface mixing ratios above the focus is predicted to become less than 600 ppm (Table 2).

3.2.2. Small leak with large surface expression

Taking the example of a very small leak, 4 g h^{-1} that is 50 cm below the surface, the calculated surface CH_4 mixing ratio is predicted to be largest when the surface roughness is smallest, (e.g. snow) the wind speed decreases, and the atmosphere becomes more stable. When all of these variables are tuned in the ESCAPE model to realistic extremes, i.e. z_0 of 0.0001 m, wind speed of 0.5 m s^{-1} and stability of PGSC G, the surface mixing ratio above the focus is predicted to exceed 16,000 ppm (Table 3).

4. Conclusion

Here, we present data showing the changing modelled and measured CH_4 mixing ratios on the surface above an underground controlled release of methane at METEC. On-site facilities were used to produce leaks of known rates from outlets beneath the surface of the ground and the resulting surface CH_4 mixing ratios were measured using the same instruments as used in pipeline walking surveys. The highest surface mixing ratios are detected directly above the leak, which exponentially decrease with distance and are not above background farther than 4.5 m from the focus. These surface measurements also show significant CH_4 mixing ratio changes in varying meteorological and micrometeorological conditions for the same leak rate. Generally, mixing ratios were higher during lower winds and non-neutral atmospheric events.

Using the measurement data presented in Table 1, the average measured surface concentration can be calculated (551, 9593 and 12,714 ppm for the 4, 20 and 80 g h^{-1} release rates, respectively) and used to calculate a dimensionless value between the measured and average measured surface concentrations that represents how much the measurement is over or underestimated. To investigate real-world utility of the dimensionless number, which indicates the relative under/over-estimate in surface concentration measurement, we can plot it against the wind speed (Fig. 6) where there is a correlation ($m = -25$; $R^2 = 0.65$). The relationship derived from this observation (Equation (9)) could be used as a simple "rule-of-thumb" by distribution network surveyors to interpret how surface concentration measurements varies with wind speed and indicates the normalized severity of the leak. Here, if a measurement took place while the wind speed was 6 m s^{-1}, the surface concentration would be a factor 0.9 less than if it were conducted during a wind speed of 2.4 m s^{-1}. From the limited measurements, the data suggests that this is generally consistent during stable, unstable and neutral conditions.

$$\frac{over}{under}estimate\ factor = -0.25\,x\,\text{Wind Speed}\ \left(\text{m}\ s^{-1}\right) + 0.6 \quad \text{(Equation 9)}$$

In parallel to the measurements, a dynamic process-based resistance

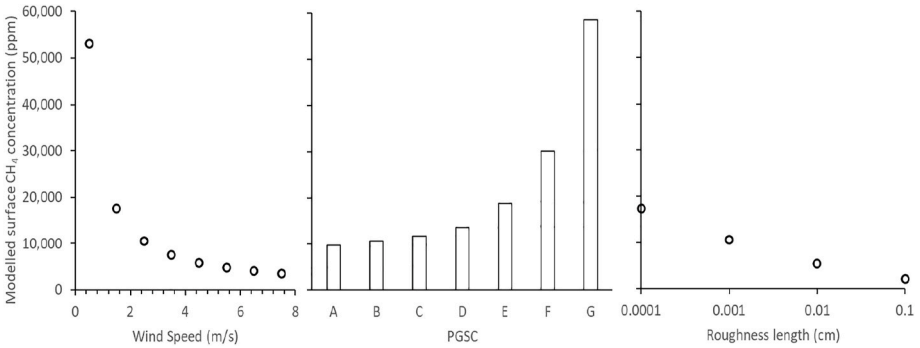

Fig. 5. Sensitivity analysis using the model to calculate surface CH_4 mixing ratios at the focus above a larger than average leak, 80 g h^{-1}. Left pane shows the effect of changing wind speed input while keeping PGSC as B, z_o at 0.001 cm. Center pane shows the effect of changing the stability input while keeping WS at 2.5 m s^{-1} and z_o at 0.001 cm. Right pane shows the effect of changing roughness length input while keeping WS at 2.5 m s^{-1} and PGSC at B.

Table 2
Sensitivity analysis using the model to calculate surface CH_4 mixing ratios at the focus above a larger than average leak, 80 g h^{-1}. The table uses the following abbreviations: WS for wind speed, PGSC for Pasquill-Gifford Stability Class, L for the Monin-Obukhov length, z_0 for roughness length and X_s for surface mixing ratio. Pairs of lines reflecting extreme conditions are color coded.

Scenario	WS (m/s)	PGSC	*L* (m)	z_0 (m)	*Xs* (ppm)
Base Case	2.5	B	-11	0.001	10,606
Higher wind speed	7.5	B	-11	0.001	3,537
Lower wind speed	0.5	B	-11	0.001	53,024
Very unstable	2.5	A	-1	0.001	7,131
Very stable	2.5	G	5	0.001	58,593
Smoother surface	2.5	B	-11	0.0001	17,391
Rougher surface	2.5	B	-11	0.1	2,081
Rougher surface, more wind, very unstable	7.5	A	-5	0.1	545

Table 3
Sensitivity analysis using the model to calculate surface CH_4 mixing ratios at the focus above a larger than average leak, 4 g h^{-1}. The table uses the following abbreviations: WS for wind speed, PGSC for Pasquill-Gifford Stability Class, L for the Monin-Obukhov length, z_0 for roughness length and X_s for surface mixing ratio. Pairs of lines reflecting extreme conditions are color coded, using same colors as Table 2.

Scenario	WS (m/s)	PGSC	*L* (m)	z_0 (m)	*Xs* (ppm)
Base Case	2.5	B	10	0.001	382
More wind	7.5	B	10	0.001	129
Less wind	0.5	B	10	0.001	1,143
Very unstable	2.5	B	-5	0.001	441
Very stable	2.5	G	5	0.001	2,665
Smoother surface	2.5	B	-11	0.0001	792
Rougher surface	2.5	B	-11	0.1	96
Smoother surface, less wind, very stable	0.5	G	5	0.0001	16,693

ESCAPE (Estimating the Surface Concentration Above Pipeline Emissions) model was developed to calculate surface CH_4 mixing ratios above a leak using input on controlled release rate soil and meteorological conditions. The measured surface mixing ratios were used to validate ESCAPE model output. Measured CH_4 mixing ratios were in good agreement with modelled estimates at distances above the leak, R^2 of 0.95, and emissions from the surface vary with environmental conditions, in particular wind speed and atmospheric stability, which is consistent with other process-based emission models (Nemitz et al., 2000; Riddick et al., 2018; Sutton et al., 1998). However, we find the model overpredicts surface mixing ratios in stable conditions, m of 0.74 in PGSC E stability, while underpredicting in unstable conditions, m of 1.30 in PGSC B conditions. As this is a systematic error, it would suggest that the fixed values taken for the Monin-Obukhov length (*L*, m) in each

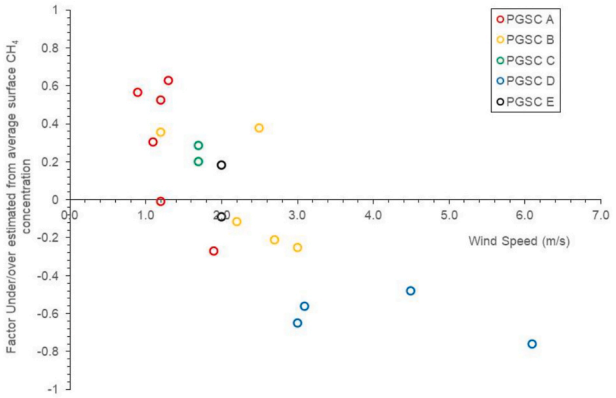

Fig. 6. The fractional difference between the measured and average measured surface concentrations plotted against the wind speed. The Pasquill Gifford Stability Classes (PGSC) are represented as colors. The average measured surface concentration was be calculated as 551, 9593 and 12,714 ppm for the 4, 20 and 80 g h^{-1} release rates, respectively.

stability class, *L* of −11 m for PGSC B and *L* of 5 m for PGSC E, could be improved by taking in-situ measurements of the micrometeorology. However, it is unlikely that a gas operator would have a sonic anemometer to hand and the ESCAPE model is intended to be a straightforward, qualitative tool that uses easily measured atmospheric conditions to assess leak severity, therefore, these model uncertainties should be noted but will not affect the overall efficacy of the tool. Accordingly, we estimate the absolute uncertainty in the modelled CH_4 surface mixing ratios at ± 30%.

4.1. Model sensitivity

Using the sensitivity analysis for large and small leaks, Tables 2 and 3 respectively, the ESCAPE model predicts that lower wind speeds will result in higher surface enhancements as aerodynamic resistance is increased due to the decreased vertical transport of the gas from the surface (Fig. 5). Periods of high stability also result in higher surface enhancements as surface air is trapped in the boundary layer. Conversely, during periods of atmospheric instability, i.e. high surface heating, the gas at the surface is readily transported from the surface to the atmosphere. However, it should be noted that while the observed surface concentrations are higher at low wind speed and high stability, the concentration increase is not substantial enough to decrease the diffusion or microbial CH_4 uptake below the surface. Therefore, just under the surface, the concentration is still very high – typically percent CH_4 – and the near-surface leak expression does not substantially change in size.

4.2. Implications for walking surveys

The most important finding of this modeling/measurement effort is that changing atmospheric conditions profoundly affects the CH_4 mixing ratios measured at the surface above an underground gas leakage. This is a finding consistent with the CH_4 concentration measurements of Chen et al. (2020) at the Munich Oktoberfest in 2018. Here we identify the wind speed, roughness length and the atmospheric stability as the environmental variables that most significantly affect surface concentration.

For small leaks (~4 g CH_4 h^{-1}), surface enhancements could appear much larger than expected. High surface enhancements above small leaks are predicted to occur during very stable events with low wind speeds (Fig. 7A). As these low wind, high stability events generally occur during the night and early morning, it is reasonable to assume that these conditions are unlikely to be encountered during pipeline walking surveys. Using meteorological data from the Christman Field meteorological station (public station near METEC) in the ESCAPE model with a leak of 4 g h^{-1}, we estimate that there were 206 h in 2019 where ground mixing ratios above the leak would exceed 10,000 ppm. Even though these leaks are exceedingly small, mercaptan can be detected by the human nose at mixing ratios of around 100 ppm and the gas from these leaks would be overwhelmingly detectable during these low wind, stable atmospheric events. Small, recurrent, untraceable leaks have been encountered by many fire departments and continue to be reported by the public even though the source cannot be located and the leak repaired (M. Housley, Poudre Fire Authority, CO, USA, pers. comm.). However, all of these were at night and unlikely to be observed. Despite this, it should be acknowledged that even small leaks from pipelines could result in explosive atmospheres in conditions where gas migrates into enclosed spaces, typically without atmospheric transport.

Of more concern is the potential misclassification of large leaks (e.g. > 80 g CH_4 h^{-1}). The ESCAPE model output predicts that in higher wind and unstable atmospheric conditions, CH_4 surface mixing ratios could be significantly underestimated by up to a factor of 20 and appear very small (Fig. 7B). As these conditions would occur during the day when survey teams are likely to be working, this misidentification presents a potential safety hazard. Again, using meteorological data from the Christman Field meteorological station in the model with a leak of 80 g h^{-1}, we estimate the maximum surface CH_4 mixing ratios would have been less than 10,000 ppm for 383 h in 2019. All of these were during the day in conditions walking survey teams are likely to be working and could have resulted in a mis-classification of risk when a leak is found, or near-surface mixing ratios small enough to elude detection altogether. It should be noted that, based on Christman Field meteorological data, the ESCAPE model predicts surface mixing ratios higher than the lower explosive limit (LEL) for methane for 1358 h in 2019, or 16% of the year.

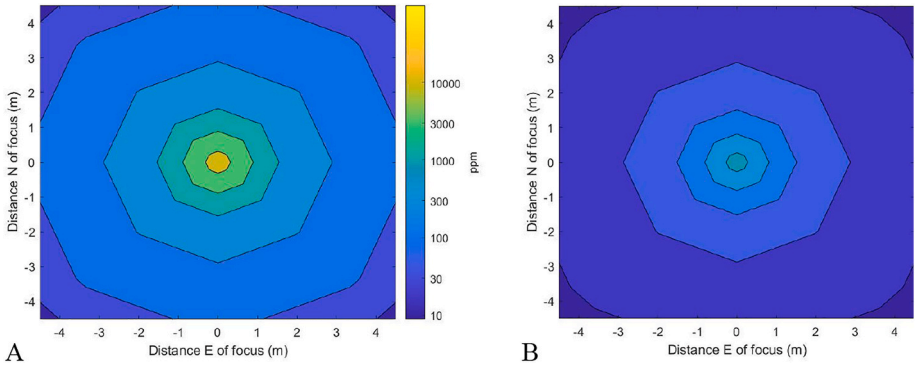

Fig. 7. Modelled surface methane mixing ratios above a leak 50 cm below the ground for A) a 4 g CH_4 h^{-1} in conditions where the surface is smoother ($z_0 = 0.0001$), with less wind (u = 0.5 m s^{-1}) and a very stable atmosphere (L = 5 m) and B) a 80 g CH_4 h^{-1} in conditions with a rougher surface ($z_0 = 0.1$), with more wind (u = 7.5 m s^{-1}) and an unstable atmosphere (L = −5 m) on the same mixing ratio color scale.

4.3. Future applications of the ESCAPE model

It is predicted that hydrogen gas could replace CH_4 as a fuel piped from renewable energy facilities to the end user. In contrast to CH_4, hydrogen is explosive at a greater range of concentrations, i.e. between 4 and 75%. This means that if CH_4 collects in an enclosed space it will be explosive over a smaller range of concentrations than the same gas intrusion by hydrogen, indicating that hydrogen may present a greater hazard than CH_4 under similar leak conditions, and that the detection, quantification and repair of hydrogen leaks would be more important than natural gas leaks. With further field testing with hydrogen, the ESCAPE model could also be used to quantify hydrogen leaks from above surface concentrations.

5. Discussion

This study highlights the importance of the meteorological and micrometeorological effects on the transport of gas from the surface to the atmosphere, where interplay between the soil surface conditions (roughness) and the atmospheric conditions (turbulence and stability) have the largest effect on the flux. Increased wind speed and high stability decrease atmospheric resistance, resulting in increased vertical transport which decreases the surface concentration. Therefore, threshold meteorological/micrometeorological conditions exist where gas exchange in the soil is less than the vertical transport and not able to maintain replenishment of the gas to the surface, resulting in smaller than expected surface enhancements.

For larger gas leaks, it is possible that vertical atmospheric transport occurs fast enough to remove CH_4 to the atmosphere, which could result in a walking survey classifying the leak at a lower risk level or missing the leak entirely, and the source remaining undetected or scheduled at low priority for repair. Conversely, in low wind, stable conditions, CH_4 from smaller leaks can collect at the surface in enhancements high enough to become explosive. Both scenarios present a hazard, and this study highlights the importance of understanding the relative effects of above surface gas transport on gas emitted from an underground pipeline leak. Taking the previous example, where the leak in Fig. 6A is 4 g CH_4 h^{-1} while the leak in Fig. 6B 80 g CH_4 h^{-1}, the reasonable conclusion is that the smaller leak should be repaired before the larger. However, the larger leak can more often result in a hazardous scenario and without considering the meteorology could easily be misidentified as less dangerous.

To improve industry best practices, we make the following recommendations:

- The surveyor should record the meteorological conditions at the time of the leak detection.
- To improve the chance of detecting small leaks, surveys should be performed on days of atmospheric stability and where winds are low (<1.5 m s^{-1}).
- To avoid misclassifying leaks or missing detections all together surveys should not be performed on days where there are strong winds or strong solar irradiance.
- Known leak locations (e.g. PHMSA class II and III) should be revisited and measured in different conditions to verify the leak is classified in the proper risk level.

In the bigger picture, mitigating CH_4 emissions from the gas distribution network are sensible, cost-effective and economically realistic if the Paris Agreement is to be met (Nisbet et al., 2019). If time, effort and money can be directed by the output of ESCAPE model to correctly identify and repair the largest distribution leaks (Nisbet et al., 2020), the majority of the 630,000 leaks in the U.S. distribution mains could be mitigated and reduce the overall atmospheric CH_4 emissions by 0.69 Tg each year (Weller et al., 2020), which may go some way to bringing emissions from this sector back to the direction set out by the Paris goals.

Author contributions

S. N. R. conceived and designed the study, conducted experiments, conducted formal analysis and wrote the original draft, C. B. was responsible conducting experiments, reviewing and editing, A. D. was responsible conducting experiments, reviewing and editing, T.V. was responsible conducting experiments, reviewing and editing, K. S. was responsible for funding acquisition, reviewing and editing, Y. C. validated results, K. B. was responsible for funding acquisition, reviewing and editing and D. Z. was responsible for funding acquisition, supervision, validation, reviewing and editing.

Declaration of competing interest

The authors declare that they have no known competing financial interests or personal relationships that could have appeared to influence the work reported in this paper.

Acknowledgements

This material is based upon work supported by the US Department of Transportation (DOT) Pipeline and Hazardous Materials Safety Administration (PHMSA) under grant numbers 693JK31810013 and 693JK32010011.

References

Bell, C.S., Vaughn, T., Zimmerle, D., 2020. Evaluation of next generation emission measurement technologies under repeatable test protocols. Elem. Sci. Anth. 8, 32. https://doi.org/10.1525/elementa.426.

Bu, F., Liu, Yang, Liu, Yongbin, Xu, Z., Chen, S., Jiang, M., Guan, B., 2021. Leakage diffusion characteristics and harmful boundary analysis of buried natural gas pipeline under multiple working conditions. J. Nat. Gas Sci. Eng. https://doi.org/10.1016/j.jngse.2021.104047, 104047.

Chen, J., Dietrich, F., Maazallahi, H., Forstmaier, A., Winkler, D., Hofmann, M.E.G., Denier van der Gon, H., Röckmann, T., 2020. Methane emissions from the Munich oktoberfest. Atmos. Chem. Phys. 20, 3683–3696. https://doi.org/10.5194/acp-20-3683-2020.

Cho, Y., Ulrich, B.A., Zimmerle, D.J., Smits, K.M., 2020. Estimating natural gas emissions from underground pipelines using surface concentration measurements☆. Environ. Pollut. 267, 115514. https://doi.org/10.1016/j.envpol.2020.115514.

Defratyka, S.M., Paris, J.-D., Yver-Kwok, C., Fernandez, J.M., Korben, P., Bousquet, P., 2021. Mapping urban methane sources in Paris, France. Environ. Sci. Technol. 55, 8583–8591. https://doi.org/10.1021/acs.est.1c00859.

Dlugokencky, E.J., 2020. Trends in Atmospheric Methane. NOAA/GML. Global CH4 Monthly Means.

Henrie, M., Nicholas, R.E., Carpenter, P., 2016. Pipeline Leak Detection Handbook. Elsevier. https://doi.org/10.1016/C2014-0-01914-4.

Hou, Z., Yuan, X., 2021. Leakage locating and sampling optimization of small-rate leakage on medium-and-low-pressure unground natural gas pipelines. J. Nat. Gas Sci. Eng. 94, 104112. https://doi.org/10.1016/j.jngse.2021.104112.

Jury, W.A., Gardner, W.R., Gardner, W.H., 1991. Soil Physics, fifth ed. J. Wiley, New York.

Lamb, B.K., Edburg, S.L., Ferrara, T.W., Howard, T., Harrison, M.R., Kolb, C.E., Townsend-Small, A., Dyck, W., Possolo, A., Whetstone, J.R., 2015. Direct measurements show decreasing methane emissions from natural gas local distribution systems in the United States. Environ. Sci. Technol. 49, 5161–5169. https://doi.org/10.1021/es505116p.

Maazallahi, H., Fernandez, J.M., Menoud, M., Zavala-Araiza, D., Weller, Z.D., Schwietzke, S., von Fischer, J.C., Denier van der Gon, H., Röckmann, T., 2020. Methane mapping, emission quantification, and attribution in two European cities: utrecht (NL) and Hamburg (DE). Atmos. Chem. Phys. 20, 14717–14740. https://doi.org/10.5194/acp-20-14717-2020.

Mitton, M., 2018. Subsurface Methane Migration from Natural Gas Distribution Pipelines as Affected by Soil Heterogeneity: Field Scale Experimental and Numerical Study. Colorado School of Mines.

Neirynck, J., Kowalski, A.S., Carrara, A., Genouw, G., Berghmans, P., Ceulemans, R., 2007. Fluxes of oxidised and reduced nitrogen above a mixed coniferous forest exposed to various nitrogen emission sources. Environ. Pollut. 149, 31–43. https://doi.org/10.1016/j.envpol.2006.12.029.

Nemitz, E., Sutton, M.A., Schjoerring, J.K., Husted, S., Paul Wyers, G., 2000. Resistance modelling of ammonia exchange over oilseed rape. Agric. For. Meteorol. 105, 405–425. https://doi.org/10.1016/S0168-1923(00)00206-9.

Nisbet, E.G., Fisher, R.E., Lowry, D., France, J.L., Allen, G., Bakkaloglu, S., Broderick, T. J., Cain, M., Coleman, M., Fernandez, J., Forster, G., Griffiths, P.T., Iverach, C.P., Kelly, B.F.J., Manning, M.R., Nisbet-Jones, P.B.R., Pyle, J.A., Townsend-Small, A., al-Shalaan, A., Warwick, N., Zazzeri, G., 2020. Methane mitigation: methods to reduce

emissions, on the path to the Paris agreement. Rev. Geophys. 58 https://doi.org/10.1029/2019RG000675.

Nisbet, E.G., Manning, M.R., Dlugokencky, E.J., Fisher, R.E., Lowry, D., Michel, S.E., Myhre, C.L., Platt, S.M., Allen, G., Bousquet, P., Brownlow, R., Cain, M., France, J.L., Hermansen, O., Hossaini, R., Jones, A.E., Levin, I., Manning, A.C., Myhre, G., Pyle, J. A., Vaughn, B.H., Warwick, N.J., White, J.W.C., 2019. Very strong atmospheric methane growth in the 4 Years 2014–2017: implications for the Paris agreement. Global Biogeochem. Cycles 33, 318–342. https://doi.org/10.1029/2018GB006009.

PHMSA, 2021. Distribution, Transmission & Gathering, LNG, and Liquid Accident and Incident Data. Pipeline and Hazardous Materials Safety Administration.

Riddick, S.N., Blackall, T.D., Dragosits, U., Tang, Y.S., Moring, A., Daunt, F., Wanless, S., Hamer, K.C., Sutton, M.A., 2017. High temporal resolution modelling of environmentally-dependent seabird ammonia emissions: description and testing of the GUANO model. Atmos. Environ. 161, 48–60. https://doi.org/10.1016/j.atmosenv.2017.04.020.

Riddick, S.N., Dragosits, U., Blackall, T.D., Tomlinson, S.J., Daunt, F., Wanless, S., Hallsworth, S., Braban, C.F., Tang, Y.S., Sutton, M.A., 2018. Global assessment of the effect of climate change on ammonia emissions from seabirds. Atmos. Environ. 184, 212–223. https://doi.org/10.1016/j.atmosenv.2018.04.038.

Seinfeld, J.H., Pandis, S.N., 2016. Atmospheric Chemistry and Physics: from Air Pollution to Climate Change, third ed. John Wiley & Sons, Inc, Hoboken, New Jersey.

Shaw, D., Phillips, M., Munoz, E., Rehma, H., Gibson, C., Mayernik, C., 2012. Leak Detection Study (Final Report No. DTPH56-11- D- 000001). U.S. Department of Transportation Pipeline and Hazardous Materials Safety Administration.

Sutton, M.A., Burkhardt, J.K., Guerin, D., Nemitz, E., Fowler, D., 1998. Development of resistance models to describe measurements of bi-directional ammonia surface–atmosphere exchange. Atmos. Environ. 32, 473–480. https://doi.org/10.1016/S1352-2310(97)00164-7.

Sutton, M.A., Flower, D., Moncriefe, J.B., 1993. The exchange of atmospheric ammonia with vegetated surfaces. I: unfertilized vegetation. Q. J. R. Meteorol. Soc. 119, 1023–1045. https://doi.org/10.1002/qj.49711951309.

Ulrich, B.A., Mitton, M., Lachenmeyer, E., Hecobian, A., Zimmerle, D., Smits, K.M., 2019. Natural gas emissions from underground pipelines and implications for leak detection. Environ. Sci. Technol. Lett. 6, 401–406. https://doi.org/10.1021/acs.estlett.9b00291.

Wang, X., Tan, Y., Zhang, T., Xiao, R., Yu, K., Zhang, J., 2021. Numerical study on the diffusion process of pinhole leakage of natural gas from underground pipelines to the soil. J. Nat. Gas Sci. Eng. 87, 103792. https://doi.org/10.1016/j.jngse.2020.103792.

Wang, Y., Hu, C., Ming, H., Oenema, O., Schaefer, D.A., Dong, W., Zhang, Y., Li, X., 2014. Methane, carbon dioxide and nitrous oxide fluxes in soil profile under a winter wheat-summer maize rotation in the north China plain. PloS One 9, e98445. https://doi.org/10.1371/journal.pone.0098445.

Weller, Z.D., Hamburg, S.P., von Fischer, J.C., 2020. A national estimate of methane leakage from pipeline mains in natural gas local distribution systems. Environ. Sci. Technol. 54, 8958–8967. https://doi.org/10.1021/acs.est.0c00437.

Zhang, H., Lindberg, S.E., Barnett, M.O., Vette, A.F., Gustin, M.S., 2002. Dynamic flux chamber measurement of gaseous mercury emission fluxes over soils. Part 1: simulation of gaseous mercury emissions from soils using a two-resistance exchange interface model. Atmos. Environ. 36, 835–846. https://doi.org/10.1016/S1352-2310(01)00501-5.

Zimmerle, D.J., Pickering, C.K., Bell, C.S., Heath, G.A., Nummedal, D., Pétron, G., Vaughn, T.L., 2017. Gathering pipeline methane emissions in Fayetteville shale pipelines and scoping guidelines for future pipeline measurement campaigns. Elem. Sci. Anthr. 5, 70. https://doi.org/10.1525/elementa.258.